

# Clinical Comparison of Cardiac Blood Pool Visualization with Technetium-99m Red Blood Cells Labeled In Vivo and with Technetium-99m Human Serum Albumin

James H. Thrall, John E. Freitas, Dennis Swanson, W. Leslie Rogers, Jean M. Clare,  
Manuel L. Brown\*, and Bertram Pitt

*University of Michigan Medical Center, Ann Arbor, Michigan*

***Technetium-99m red blood cells (Tc-RBC) labeled by an in vivo technique were compared with two preparations of Tc-99m human serum albumin (HSA) for cardiac blood-pool imaging. Relative distribution of the tracers was analyzed on end-diastolic frames of gated blood-pool studies and on whole-body (head to mid-thigh) anterior pinhole images.***

***The Tc-RBC demonstrated greater relative percentage localization in the cardiac blood pool, higher target-to-background ratios in the left ventricle, and less liver concentration. For cardiac blood-pool imaging, Tc-RBC labeled by the in vivo approach appears to be superior to the two Tc-HSA preparations studied.***

**J Nucl Med 19: 796-803, 1978**

Dynamic imaging of the cardiac blood pool to analyze regional myocardial motion and to calculate the ejection fraction has become increasingly important in myocardial disease, both in the initial diagnosis and in the serial evaluation of therapeutic interventions (1-4). Fundamental to the procurement of high-quality blood-pool studies is the use of a suitable radiopharmaceutical that remains within the vascular space.

There are two major categories of tracers available for blood-pool imaging: labeled red blood cells (RBC) and labeled human serum albumin (HSA). Recently, Pavel and associates (5) have described an in vivo procedure for RBC labeling with [<sup>99m</sup>Tc] pertechnetate. The in vivo approach affords several distinct advantages over in vitro methods of labeling RBC (6,7) and potential advantages over the use of HSA. Preliminary data obtained from serial blood sampling indicates that the in vivo approach provides good initial labeling efficiency, with the recovered activity remaining in the red-cell fraction for prolonged periods, allowing blood-pool images of good quality to be readily obtained (5,8,9).

We have undertaken a prospective study to evaluate imaging of the cardiac blood pool with technetium-99m red blood cells (Tc-RBC) labeled by the

in vivo approach, compared with two preparations of Tc-99m human serum albumin (Tc-HSA).

## MATERIALS AND METHODS

**Radiopharmaceutical preparation.** Tc-HSA was prepared using both a commercial stannous kit\* and a modified inhouse electrolytic procedure (10). Manufacturer's instructions were followed for preparation from the commercial kit.

For the inhouse preparation, a tin wire anode and a stainless steel wire cathode are thoroughly cleaned and rinsed, and inserted through the diaphragm of a sterile apyrogenic 10-ml shielded reaction vial. Added to this vial are: a) the desired activity of [<sup>99m</sup>Tc] pertechnetate (TcO<sub>4</sub>) and 2.6 ml of physiologic saline; b) 0.2 ml of 25% HSA†; and c) 0.85 ml of 1 N HCl. A constant current of 100 mA is then applied to the electrolytic cell for 55 sec. During electrolysis, the reaction vial is agitated gently

Received Dec. 21, 1977; revision accepted Feb. 10, 1978.

For reprints contact: James H. Thrall, University of Michigan Medical Ctr., Nuclear Medicine Sec., 1405 E. Ann St., Ann Arbor, MI 48109.

\* Present address: Manuel L. Brown, Div. of Nuclear Medicine, Mayo Clinic, Rochester, MI 55901.

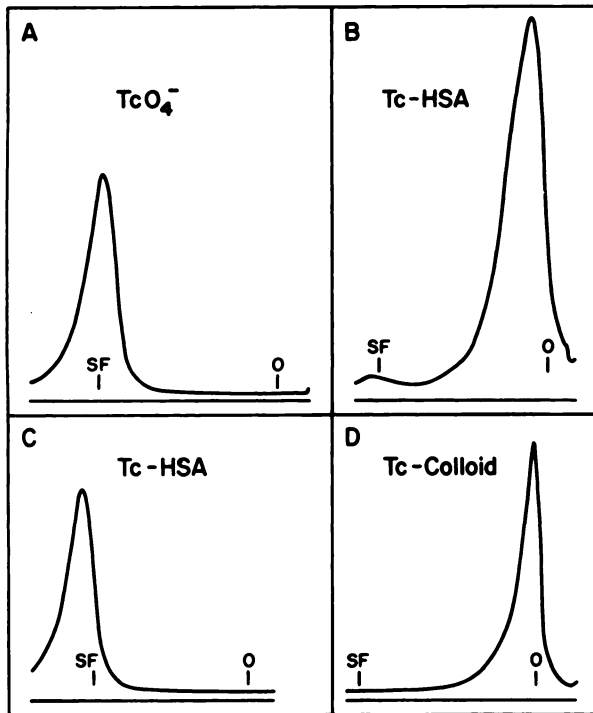


**FIG. 1.** Sample Tc-HSA chromatography.  $TcO_4^-$  (A) and Tc-HSA (B) are readily separated by conventional ITLC-SG system. In (C) and (D), ITLC-SG strips were presoaked in albumin, allowing separation of Tc-HSA from Tc-colloid.

using a circular motion. The reaction mixture is then allowed to stand at room temperature for 30 min. Following removal of the electrodes, 0.6 ml of 1 N sodium hydroxide and 0.8 ml of 8.4%  $NaHCO_3$  solution are added, buffering the preparation to a final pH of about 7.4. The product is subsequently assayed and passed through a 0.22- $\mu$  bacterial filter. The final volume is about 5 ml.

Quality-control procedures are routinely performed on all technetium radiopharmaceuticals. Sterility and pyrogen testing are done on pooled samples radiometrically and limulus lysate testing, respectively. All preparations are tested, before administration, for correct pH using narrow-range pH indicator paper. Radionuclidic and radiochemical purity of the generator eluate is ascertained before the preparation of any Tc-99m radiopharmaceutical.

Both the inhouse and the commercial-kit Tc-HSA were analyzed before injection for the presence of unreacted, unreduced  $TcO_4^-$  and colloidal forms of Tc-99m. Instant thin-layer chromatography, using silica gel (ITLC-SG) as the support medium and 85% methanol as the solvent, resulted in the separation of  $TcO_4^-$  ( $R_f = 1$ ) from Tc-HSA and colloidal Tc-99m (both  $R_f = 0$ ) (Fig. 1A, B). Because of the albumin loading effect (11) the presence of colloid was determined after presoaking ITLC-SG

strips in a physiologic saline solution of HSA (5 mg/ml) for 30 min. The strips were rinsed for 5 sec with distilled water, allowed to dry, and stored at 0–5°C until used. On presoaked ITLC-SG, using ethanol:ammonia:water (2:1:5) as the solvent,  $TcO_4^-$  and Tc-HSA migrate with an  $R_f$  of 1.0; whereas colloidal Tc-99m remains at the origin (Fig. 1C, D). This chromatography system was validated by separately analyzing the migration of  $TcO_4^-$  and that of Tc-99m colloid produced by the electrolysis method in the absence of HSA.

Patients were injected intravenously with 20 mCi of Tc-HSA in an average volume of 3.3 ml. Scanning procedures commenced within 5 min of the injection.

In vivo Tc-RBC labeling was accomplished by the method of Pavel et al. (1). A commercial kit containing stannous pyrophosphate [15.4 mg (6.3 mg  $Sn^{++}$ )] is reconstituted with 5.0 ml of 0.9% NaCl. The height and weight of the patient are obtained in order to estimate patient's blood volume from standard tables. The amount of stannous pyrophosphate to be injected is calculated by the formula:

$$\frac{\text{Patient blood volume}}{5,400 \text{ ml}} \times 2.5 \text{ ml} = \text{volume injected} \\ \text{(blood volume standard man)}$$

In no case is more than 2.5 ml (7.7 mg stannous pyrophosphate) administered. Injection is performed immediately following reconstitution.

Approximately 30 min after the injection of stannous pyrophosphate, patients receive 20 mCi  $TcO_4^-$  i.v. Scanning procedures then start within 5 min.

**Imaging methods.** For clinical studies, multiple gated blood-pool images of the heart are obtained. A format is used that provides 28 frames per cardiac cycle, and imaging is continued long enough to collect 300,000 counts per frame. A low-energy parallel-hole collimator is used on a scintillation camera with conventional field of view, interfaced to a computer. All patients are studied in both the anterior and left anterior oblique projections. The latter view is used to calculate the ejection fraction using an automated edge-detection algorithm to define regions of interest over the left ventricle (12). The images from both projections are reviewed in a dynamic-display format to analyze regional wall motion.

Fifty consecutive studies obtained with Tc-HSA (inhouse preparation) and 50 with Tc-RBC were reviewed to assess their relative quality in the dynamic-display format and to identify any factors adversely affecting the image. To determine relative quantitative tracer distribution in the field of view in clinical studies, the following calculations were

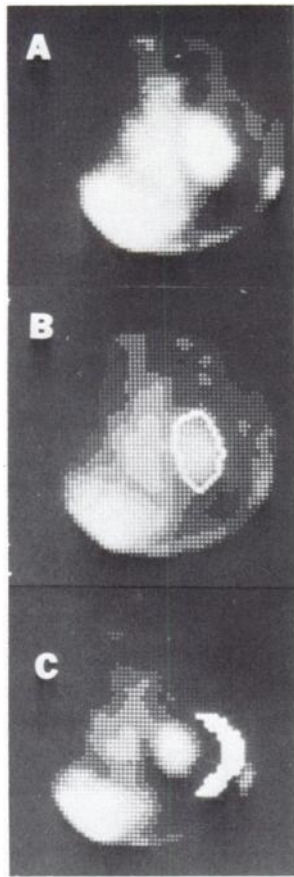


**FIG. 2.** (A) End-diastolic frame in left anterior oblique projection. (B) Computer-generated outline of left ventricle (bright dots) is used to define area of interest. (C) End-systolic frame with background area indicated by highlighted area.

made in the first 20 consecutive cases with Tc-HSA, and in the first 20 with Tc-RBC: a) net left-ventricular counts at end-diastole as a percentage of the total image count; b) average net counts per image element in the left ventricle at end-diastole; c) average background counts per image element; and d) the target-to-background ratio for the left ventricle (= average net left-ventricular counts per channel divided by average background counts per channel). All calculations were made using regions defined by an automated edge-detection algorithm (Fig. 2) on the end-diastolic frames. Background in this computer program is taken from a crescentic area lateral to the left ventricle at end-systole (Fig. 2C).

To determine the relative tracer distribution in the central blood pool, liver, and bladder with the Tc-RBC and the two HSA preparations, ten consecutive patients were imaged in the anterior projection with a pinhole aperture. The field of view in each case was from head to mid-thigh. The average subject-to-collimator distance was 120 cm. In pre-

liminary studies this field of view was shown to include over 95% of administered activity. Since the major areas of interest are in the center of the field, no field correction was made for the pinhole. The images were run for 5 min at the end of routine clinical studies (about 45 min after injection) and stored on the computer system for analysis. Regions of interest over the central blood-pool activity (heart and great vessels), the liver, and the bladder were defined with a light pen. Gross counts from each region were determined and expressed as a percentage of the total image counts to normalize between subjects.

To estimate maximum regional tracer concentrations, the maximum count in a single image element in the central blood-pool region, and another in the liver region, were determined for each of the pinhole images, and ratios between these maxima were calculated.

The Wilcoxon rank sum test (13) and Student's t-test were used respectively for statistical analysis of the pinhole and clinical study data.

## RESULTS

Chromatographic analysis of Tc-HSA prepared by electrolysis or from the commercial stannous HSA kit revealed total labeling efficiencies greater than 91% in all cases. With the electrolytic method, labeling efficiency averaged  $96.21\% \pm 1.89$  s.d. (range 94.1–99.5). Colloidal impurities in this preparation averaged  $2.13\% \pm 1.73$  s.d. (range 0.2–5.2). No colloidal impurities were detected in the commercial stannous-HSA kit, and the total labeling efficiency averaged  $94.5\% \pm 2.78$  s.d. (range 91–98.6). These results are consistent with previous reports describing in vitro analysis of Tc-HSA preparations (10,11,14–16).

Although diagnostically useful images were ob-

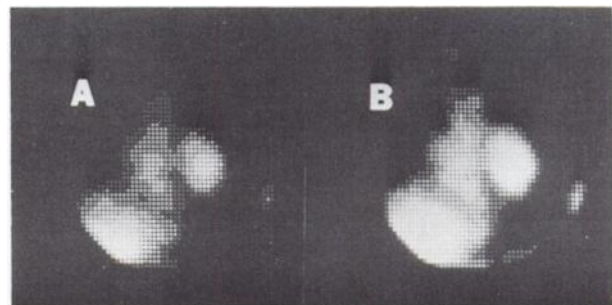


**FIG. 3.** End-diastolic frame from Tc-HSA study. In (A), computer display of heart is suboptimal because of scaling to highest-count portion of liver image. In (B), cardiac blood pool is better visualized after foreground suppression with scaling of display to highest count in heart. Display intensity was not changed.

TABLE 1. Tc-HSA AND Tc-RBC DISTRIBUTION AT END-DIASTOLE

| Case No.         | Total counts | [Net left-ventricular counts] × 100<br>total image counts | Average background counts per image element<br>(64 × 64 array) | Average net left-ventricular counts per image element<br>(64 × 64 array) | Target-to-background |
|------------------|--------------|---|--|--|----------------------|
| <b>A. Tc-HSA</b> |              |   |  |  |                      |
| 1                | 300,000      | 6.0   | 73   | 67   | .92                  |
| 2                | 300,000      | 8.0   | 84   | 59   | .70                  |
| 3                | 300,000      | 7.3   | 43   | 54   | 1.26                 |
| 4                | 300,000      | 6.5   | 56   | 57   | 1.02                 |
| 5                | 300,000      | 10.4  | 72   | 65   | .90                  |
| 6                | 300,000      | 10.4  | 41   | 97   | 2.22                 |
| 7                | 300,000      | 8.8   | 73   | 62   | .85                  |
| 8                | 300,000      | 9.3   | 68   | 69   | 1.01                 |
| 9                | 300,000      | 7.0   | 87   | 32   | .37                  |
| 10               | 300,000      | 9.4   | 65   | 56   | .86                  |
| 11               | 300,000      | 4.6   | 47   | 48   | 1.02                 |
| 12               | 300,000      | 5.1   | 64   | 51   | .80                  |
| 13               | 300,000      | 7.8   | 95   | 33   | .34                  |
| 14               | 300,000      | 10.2  | 71   | 68   | .96                  |
| 15               | 300,000      | 3.8   | 71   | 46   | .65                  |
| 16               | 300,000      | 2.0   | 83   | 49   | .59                  |
| 17               | 300,000      | 5.1   | 60   | 59   | .98                  |
| 18               | 300,000      | 5.5   | 74   | 73   | .99                  |
| 19               | 300,000      | 9.9   | 59   | 77   | 1.31                 |
| 20               | 300,000      | 5.1   | 65   | 58   | .89                  |
|                  | Mean ± s.d.  | 7.1 ± 2.41  | 67.6 ± 14.1  | 59.0 ± 14.8  | .93 ± .39            |
|                  | Range        | 2.0-10.4  | 43-95  | 32-97  | .37-2.22             |
| <b>B. Tc-RBC</b> |              |   |  |  |                      |
| 1                | 300,000      | 11.4  | 40   | 54   | 1.34                 |
| 2                | 300,000      | 11.0  | 49   | 102  | 2.09                 |
| 3                | 300,000      | 8.3   | 75   | 95   | 1.27                 |
| 4                | 300,000      | 6.2   | 87   | 76   | .87                  |
| 5                | 300,000      | 10.8  | 42   | 83   | 1.98                 |
| 6                | 300,000      | 7.6   | 36   | 78   | 2.17                 |
| 7                | 300,000      | 7.1   | 50   | 83   | 1.66                 |
| 8                | 300,000      | 5.0   | 90   | 67   | .75                  |
| 9                | 300,000      | 10.4  | 93   | 66   | .71                  |
| 10               | 300,000      | 8.7   | 76   | 67   | .89                  |
| 11               | 300,000      | 8.5   | 60   | 88   | 1.47                 |
| 12               | 300,000      | 10.2  | 59   | 52   | .88                  |
| 13               | 300,000      | 6.3   | 120  | 102  | .86                  |
| 14               | 300,000      | 8.4   | 82   | 118  | 1.44                 |
| 15               | 300,000      | 10.0  | 84   | 133  | 1.59                 |
| 16               | 300,000      | 8.1   | 95   | 83   | .87                  |
| 17               | 300,000      | 14.8  | 82   | 140  | 1.72                 |
| 18               | 300,000      | 16.3  | 105  | 130  | 1.25                 |
| 19               | 300,000      | 13.3  | 96   | 150  | 1.56                 |
| 20               | 300,000      | 6.8   | 84   | 67   | .79                  |
|                  | Mean ± s.d.  | 9.4 ± 2.80  | 75.2 ± 23.3  | 91.7 ± 29.0  | 1.31 ± .47           |
|                  | Range        | 5.0-15.3  | 36-120   | 52-150   | .71-2.17             |

tained with both types of agent, a striking difference was observed in the qualitative appearance of the Tc-RBC images compared with Tc-HSA images. With Tc-RBC, the liver had consistently less activity, relative to the cardiac blood pool, than was noted with either Tc-HSA preparation. When liver activity was significantly greater than cardiac blood-pool activity in the Tc-HSA images, the computer's display was adversely affected as a result of scaling to the

highest channel count in the image; this required foreground suppression for optimum viewing of the cardiovascular structures (Fig. 3).

In the left anterior oblique images, the net end-diastolic activity in the left ventricle, as a percentage of total image counts, averaged  $9.4 \pm 2.80$  s.d. with Tc-RBC and  $7.1 \pm 2.41$  s.d. with Tc-HSA ( $p < 0.01$ , Table 1). The left-ventricular target-to-background ratios averaged  $1.31 \pm 0.47$  for the Tc-RBC

TABLE 2. ACTIVITY DISTRIBUTION BY PINHOLE IMAGING

| Case No.                  | Central blood-pool count | Liver counts       | Central blood-pool counts | Maximum counts per channel — central blood pool | Bladder counts     |     |
|---------------------------|--------------------------|--------------------|---------------------------|---|--------------------|-----|
|                           | total image counts       | total image counts | liver counts              | Maximum counts per channel — liver              | total image counts |     |
| Tc-99m HSA (NEN)          | 1                        | .13                | .19                       | .69   | .89                | .02 |
|                           | 2                        | .08                | .23                       | .35   | .77                | .03 |
|                           | 3                        | .10                | .14                       | .71   | .89                | .05 |
|                           | 4                        | .14                | .12                       | 1.13  | 1.0                | .02 |
|                           | 5                        | .13                | .14                       | .94   | 1.08               | .06 |
|                           | 6                        | .12                | .20                       | .57   | 1.07               | .08 |
|                           | 7                        | .13                | .17                       | .79   | .92                | .09 |
|                           | 8                        | .11                | .20                       | .56   | .94                | .01 |
|                           | 9                        | .14                | .16                       | .90   | .86                | .02 |
|                           | 10                       | .23                | .35                       | .66   | .99                | .01 |
| Tc-99m HSA (electrolytic) | 11                       | .16                | .19                       | .81   | 1.15               | .04 |
|                           | 12                       | .10                | .13                       | .77   | .92                | .04 |
|                           | 13                       | .15                | .13                       | 1.20  | 1.48               | .03 |
|                           | 14                       | .13                | .20                       | .68   | .97                | .01 |
|                           | 15                       | .13                | .15                       | .87   | 1.18               | .05 |
|                           | 16                       | .10                | .20                       | .47   | .96                | .05 |
|                           | 17                       | .16                | .31                       | .51   | .79                | .03 |
|                           | 18                       | .20                | .23                       | .88   | 1.01               | .01 |
|                           | 19                       | .17                | .12                       | 1.46  | 1.55               | .02 |
|                           | 20                       | .15                | .14                       | 1.06  | 1.29               | .07 |
| Tc-99m RBC                | 21                       | .20                | .13                       | 1.52  | 1.44               | .07 |
|                           | 22                       | .27                | .09                       | 3.14  | 2.73               | .04 |
|                           | 23                       | .15                | .10                       | 1.50  | 2.26               | .04 |
|                           | 24                       | .19                | .06                       | 3.04  | 2.30               | .01 |
|                           | 25                       | .21                | .11                       | 1.96  | 2.64               | .01 |
|                           | 26                       | .31                | .15                       | 2.10  | 2.46               | .01 |
|                           | 27                       | .19                | .15                       | 1.31  | 2.02               | .07 |
|                           | 28                       | .36                | .12                       | 2.94  | 4.27               | .02 |
|                           | 29                       | .21                | .16                       | 1.28  | 1.71               | .02 |
|                           | 30                       | .20                | .13                       | 1.56  | 1.94               | .02 |
| Tc-99m HSA (NEN)          |                          |                    |                           |   |                    |     |
| Mean ± s.d.               | .13 ± .04                | .19 ± .07          | .73 ± .22                 | .94 ± .10                                       | .04 ± .03          |     |
| Range                     | .08–.23                  | .12–.35            | .35–1.13                  | .77–1.08  | .01–.09            |     |
| Tc-99m HSA (electrolytic) |                          |                    |                           |   |                    |     |
| Mean ± s.d.               | .15 ± .03                | .18 ± .06          | .87 ± .30                 | 1.13 ± .25                                      | .03 ± .02          |     |
| Range                     | .10–.20                  | .12–.31            | .47–1.46                  | .79–1.55  | .01–.07            |     |
| Tc-99m RBC                |                          |                    |                           |   |                    |     |
| Mean ± s.d.               | .24 ± .06                | .12 ± .03          | 2.04 ± .74                | 2.38 ± .78                                      | .03 ± .02          |     |
| Range                     | .15–.36                  | .06–.16            | 1.31–3.14                 | 1.44–4.27                                       | .01–.07            |     |

and averaged  $0.93 \pm 0.39$  s.d. for studies with Tc-HSA ( $p < 0.01$ , Table 1).

The pinhole images showed 24% of the total activity concentrated in the central blood pool for Tc-RBC, compared with an average of only 14% for Tc-HSA (Table 2). At the same time, fractional liver activity was 50% greater for Tc-HSA. These differences in activity were highly significant for both regions ( $p < 0.01$ ). The observation of increased blood-pool activity and reduced liver activity for Tc-RBC is in agreement with the clinical image data

but direct numerical comparison cannot be made due to differences in the fields of view. No differences were observed in the bladder regions.

The quantitative differences in relative distribution are readily appreciated by inspection of the pinhole images. Figures 4, 5, and 6 illustrate representative cases obtained with each of the three preparations, with corresponding isometric displays. In the albumin images (Figs. 5, 6), the large second peak seen in the isometric displays is due to the high liver activity.

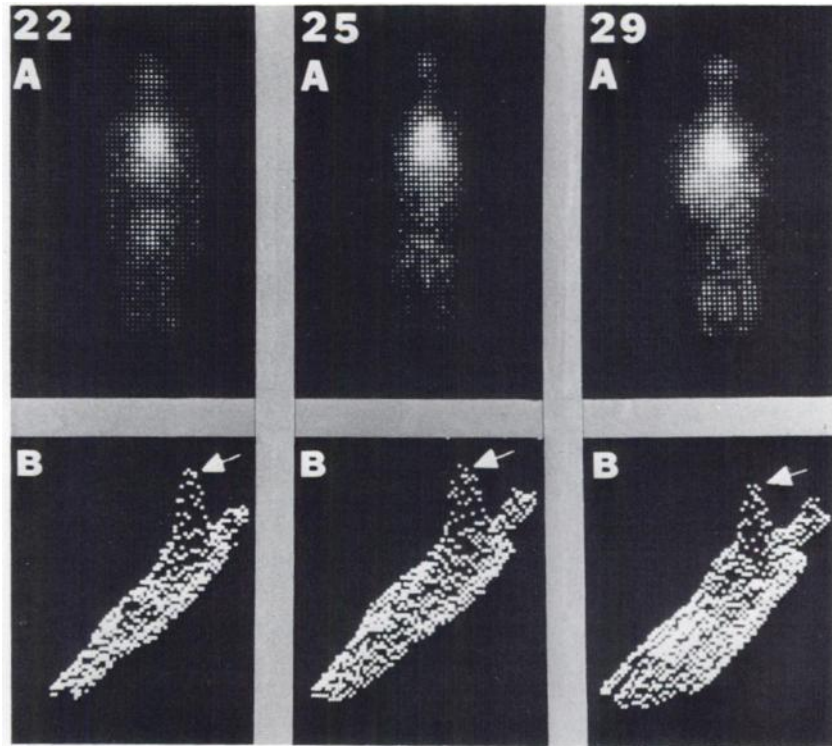


**FIG. 4.** Whole-body pinhole images (A) and isometric displays (B) from selected cases with Tc-RBC. Note single large peak in isometric displays for cardiac blood pool. (Numbers refer to case numbers from Table 2).

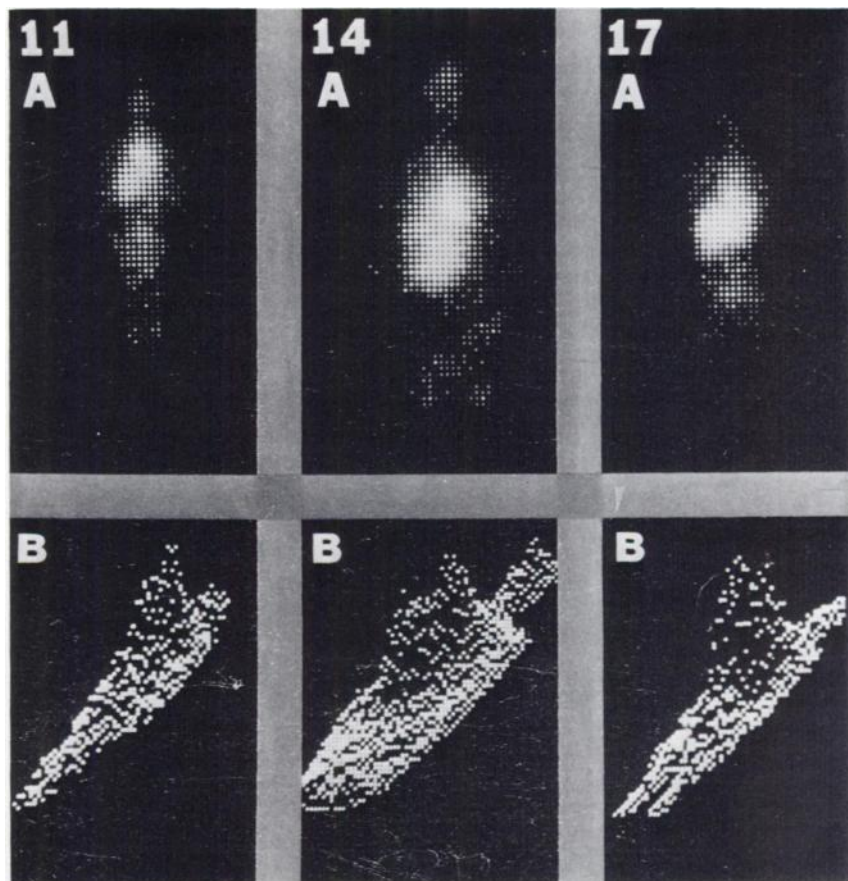


**FIG. 5.** Whole-body pinhole images with inhouse Tc-HSA preparation. Note second large peak in isometric display, due to liver activity.

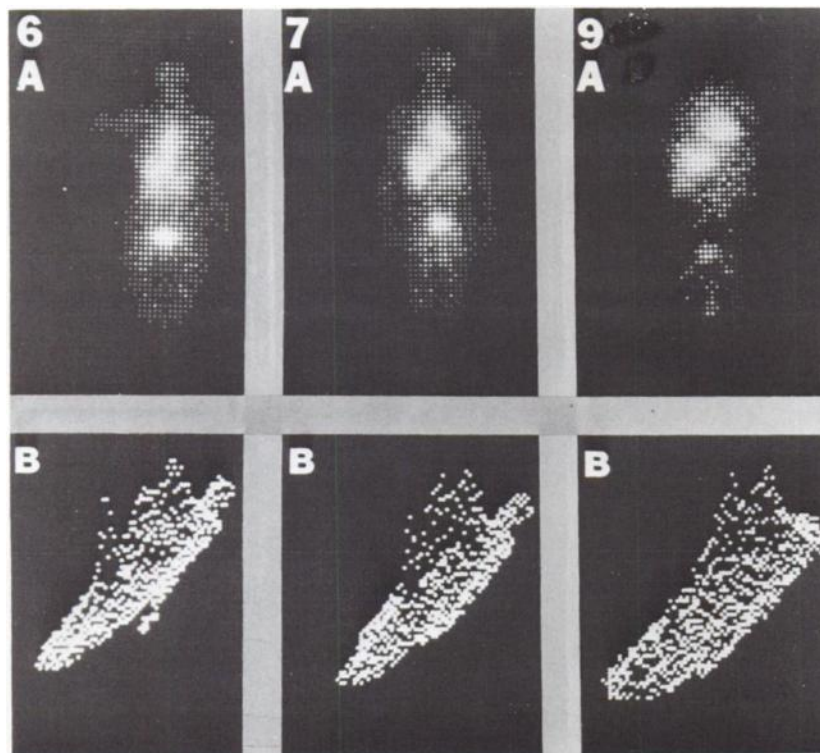


**FIG. 6.** Whole-body pinhole images with stannous-HSA kit. Note again double peaking in isometric display, due to liver activity.

#### DISCUSSION

Several investigators have suggested that Tc-RBC might be superior to Tc-HSA for cardiac blood-pool imaging because of the *in vivo* stability of Tc-RBC and the observation that albumin leaks from the vascular space with time (5,6,16,17). Such leakage reduces effective tracer activity and the target-to-background ratio. Although we did not document the leakage problem directly by obtaining serial blood samples, the lower heart-to-background ratios achieved with Tc-HSA, as compared with Tc-RBC, are an indicator of this phenomenon.

We attempted to explain the marked liver uptake of the Tc-HSA preparations by chromatographic analysis to detect Tc-colloids or other reduced-Tc contaminants that would be actively taken up by the liver. Both Tc-HSA preparations, however, demonstrated good *in vitro* labeling efficiencies. The small amount of Tc-colloid detected chromatographically is not sufficient to explain the marked liver activity with Tc-HSA, and confirms the observations of Rhodes that conventional *in vitro* procedures are not always good predictors of *in vivo* behavior (16).

The marked Tc-HSA liver activity may be due to *in vivo* loss of the Tc-99m label with subsequent hydrolysis to colloid, but it is more likely the result of HSA denaturation at the acidic pH used in the labeling procedures. Although the exact mechanism is still not known, it is obvious that whole-body imag-

ing provides a useful additional method of analyzing tracers by allowing direct comparison of their actual *in vivo* distribution in the clinical setting.

The differences in *in vivo* localization of Tc-RBC and Tc-HSA have technical implications and directly affect the quality of cardiac blood-pool imaging. The greater count rate in the heart's blood pool is an advantage of Tc-RBC over Tc-HSA: it reduces imaging time for equivalent statistical accuracy in delineating the left ventricle. It must be stressed that this may not be appreciated if one considers the total count rate in the detector's field of view. If only the photons arising in the area of diagnostic interest (i.e., left ventricle) are considered, however, the data indicate that the useful count rate with Tc-RBC is greater per mCi of administered activity. The higher target-to-background ratio achieved with Tc-RBC facilitates the application of automated edge-detection algorithms, which have become useful in calculating the ejection fraction.

A less obvious but important consideration is the effect of "out-of-view" activity on the energy spectrum and on the total events that the gamma camera is required to process. Any increased liver activity with Tc-HSA increases the number of internally scattered Compton photons in the image, with concomitant loss of contrast. Also, camera deadtime losses are increased relative to the useful count rate because of the greater integral count rate.

Another direct advantage of the in vivo approach to Tc-RBC labeling is that it allows use of small-volume, high-concentration bolus injections that facilitate "first pass" studies performed in conjunction with equilibrium imaging. In the RBC labeling technique, the injected volume of radioactivity is dependent only on the specific concentration of the generator eluate. In the case of the HSA radiopharmaceuticals, the volume of injection is dependent on both the eluate concentration and the volume requirements of the involved preparation. The commercial stannous-HSA kit used in the study requires a minimum volume of 2 ml for reconstitution, and the electrolytic procedure results in a final volume of 5 ml.

Two disadvantages of the in vivo Tc-RBC procedure are the inability to confirm whether the initial "cold" pyrophosphate injection has been extravasated and the requirement for two separate injections 30 min apart.

In a small series reported by Stokely et al. (18), in vivo Tc-RBC labeling was insufficient for clinical blood-pool imaging in two of 22 patients when  $^{99m}\text{Tc}$  pertechnetate was administered 24–48 hr after Tc-99m stannous pyrophosphate. In the cases included in the current study and in over 200 subsequent cases with in vivo Tc-RBC, however, we have not encountered a failure to achieve clinically useful labeling; nor did Pavel et al. note such a labeling problem in their first 75 studies (5). The 24–48 hr delay and the difference in the form of pyrophosphate administered may account for Stokely's results (18).

The results of this study suggest that Tc-RBC labeled by the in vivo technique is a superior cardiac blood-pool imaging agent compared with the two Tc-HSA preparations studied. Tc-RBC demonstrates greater cardiac blood-pool activity levels and superior target-to-background ratios, and should become the agent of choice, among the radiotracers examined, for cardiac blood-pool studies.

#### FOOTNOTES

- \* Cardiolite, New England Nuclear Corp., Boston, Mass.
- † Hyland, Costa Mesa, Calif.
- ‡ Technescan PYP, Mallinckrodt.
- || BACTEC, Johnston Laboratories, Inc., Cockeysville, Md.

#### REFERENCES

1. BORER JS, BACHARACH SL, GREEN MV, et al: Real-time radionuclide cineangiography in the noninvasive evaluation of global and regional left ventricular function at rest and during exercise in patients with coronary-artery disease. *N Eng J Med* 296: 839–844, 1977
2. PITT B, STRAUSS HW: Myocardial perfusion imaging and gated cardiac blood pool scanning: Clinical application. *Am J Cardiol* 38: 739–746, 1976
3. PIERSON RN, ALAM S, KEMP HG, et al: Radiocardiography in clinical cardiology. *Semin Nucl Med* VII: 85–100, 1977
4. STRAUSS HW: Cardiovascular nuclear medicine: A new look at an old problem. *Radiology* 121: 257–268, 1976
5. PAVEL DG, ZIMMER AM, PATTERSON VN: In vivo labeling of red blood cells with  $^{99m}\text{Tc}$ : A new approach to blood pool visualization. *J Nucl Med* 18: 305–308, 1977
6. SMITH TD, RICHARDS P: A simple kit for the preparation of  $^{99m}\text{Tc}$ -labeled red blood cells. *J Nucl Med* 17: 216–132, 1976
7. RYO UY, MOHAMMALZADEH AA, SIDDIQUI A, et al: Evaluation of labeling procedures and in vivo stability of  $^{99m}\text{Tc}$ -red blood cells. *J Nucl Med* 17: 133–136, 1976
8. COLOMBETTI LG, SIDDIQUI A: Efficiency of in vivo labeling of red blood cells with  $^{99m}\text{Tc}$ . *Nuclear Medizin* 15: 211–213, 1976
9. HAMILTON RG, ALDERSON PO: A comparative evaluation of techniques for rapid and efficient in vivo labeling of red blood cells with [ $^{99m}\text{Tc}$ ] pertechnetate. *J Nucl Med* 18: 1010–1013, 1977
10. DWORKIN HJ, GUTKOWSKI RF: Rapid closed-system production of  $^{99m}\text{Tc}$ -albumin using electrolysis. *J Nucl Med* 12: 562–565, 1971
11. LIN MS, KRUSE SL, GOODWIN DA, et al: Albumin-loading effect: A pitfall in saline paper analysis of  $^{99m}\text{Tc}$ -albumin. *J Nucl Med* 15: 1018–1020, 1974
12. BELL MR: Oak Ridge National Laboratory Technical Memo 5222.
13. HOLLANDER M, WOLFE DA: Nonparametric statistical methods. New York, John Wiley and Sons, 1973, pp 68, 282
14. MCLEAN JR, WELSH WJ: Measurement of unbound  $^{99m}\text{Tc}$  in  $^{99m}\text{Tc}$ -labeled human serum albumin. Letter to the Editor. *J Nucl Med* 17: 758–759, 1976
15. LAMSON M, CALLAHAN RJ, CASTRONOVO FP, et al: Reply to Letter to the Editor. *J Nucl Med* 17: 759, 1976
16. RHODES BA: Considerations in radiolabelling of albumin. *Semin Nucl Med* 4: 281–293, 1974
17. BLAHD WH: Nuclear Medicine. New York, McGraw-Hill, 1965, pp 598–610
18. STOKELY EM, PARKEY RW, BONTE FJ, et al: Gated blood pool imaging following  $^{99m}\text{Tc}$  stannous pyrophosphate imaging. *Radiology* 120: 433–434, 1976